
Physical Sciences Publications

Physical Sciences

2010-06-10

Veritas 2008-2009 Monitoring Of The Variable Gamma-Ray Source M 87

P. T. Reynolds
Cork Institute of Technology

Et. al.

Follow this and additional works at: <https://sword.cit.ie/dptphysciart>



Part of the [Astrophysics and Astronomy Commons](#)

Recommended Citation

Acciari, V. A. et al. (2010) 'VERITAS 2008-2009 MONITORING OF THE VARIABLE GAMMA-RAY SOURCE M 87', *The Astrophysical Journal*, 716(1), pp. 819–824. doi: 10.1088/0004-637X/716/1/819.

This Article is brought to you for free and open access by the Physical Sciences at SWORD - South West Open Research Deposit. It has been accepted for inclusion in Physical Sciences Publications by an authorized administrator of SWORD - South West Open Research Deposit. For more information, please contact sword@cit.ie.

VERITAS 2008–2009 MONITORING OF THE VARIABLE GAMMA-RAY SOURCE M 87

V. A. ACCIARI¹, E. ALIU², T. ARLEN³, T. AUNE⁴, M. BEILICKE⁵, W. BENBOW¹, D. BOLTUCH⁶, S. M. BRADBURY⁷, J. H. BUCKLEY⁵, V. BUGAEV⁵, K. BYRUM⁸, A. CANNON⁹, A. CESARINI¹⁰, Y. C. CHOW³, L. CIUPIK¹¹, P. COGAN¹², W. CUI¹³, R. DICKHERBER⁵, C. DUKE¹⁴, J. P. FINLEY¹³, G. FINNEGAN¹⁵, P. FORTIN^{2,28}, L. FORTSON¹¹, A. FURNISS⁴, N. GALANTE¹, D. GALL¹³, G. H. GILLANDERS¹⁰, S. GODAMBE¹⁵, J. GRUBE⁹, R. GUENETTE¹², G. GYUK¹¹, D. HANNA¹², J. HOLDER⁶, C. M. HUI¹⁵, T. B. HUMENSKY¹⁶, A. IMRAN¹⁷, P. KAARET¹⁸, N. KARLSSON¹¹, M. KERTZMAN¹⁹, D. KIEDA¹⁵, A. KONOPELKO²⁰, H. KRAWCZYNSKI⁵, F. KRENNRICH¹⁷, M. J. LANG¹⁰, S. LEBOHEC¹⁵, G. MAIER^{12,29}, S. MCARTHUR⁵, A. MCCANN¹², M. MCCUTCHEON¹², J. MILLIS^{21,30}, P. MORIARTY²², R. A. ONG³, A. N. OTTE⁴, D. PANDEL¹⁸, J. S. PERKINS¹, A. PICHEL²³, M. POHL^{17,31}, J. QUINN⁹, K. RAGAN¹², L. C. REYES²⁴, P. T. REYNOLDS²⁵, E. ROACHE¹, H. J. ROSE⁷, A. C. ROVERO²³, M. SCHROEDTER¹⁷, G. H. SEMBROSKI¹³, G. DEMET SENTURK²⁶, A. W. SMITH⁸, D. STEELE^{11,32}, S. P. SWORDY¹⁶, M. THEILING¹, S. THIBADEAU⁵, A. VARLOTTA¹³, S. VINCENT¹⁵, R. G. WAGNER⁸, S. P. WAKELY¹⁶, J. E. WARD⁹, T. C. WEEKES¹, A. WEINSTEIN³, T. WEISGARBER¹⁶, D. A. WILLIAMS⁴, S. WISSEL¹⁶, M. WOOD³, B. ZITZER¹³, D. E. HARRIS²⁷, AND F. MASSARO²⁷

¹ Fred Lawrence Whipple Observatory, Harvard-Smithsonian Center for Astrophysics, Amado, AZ 85645, USA

² Department of Physics and Astronomy, Barnard College, Columbia University, NY 10027, USA

³ Department of Physics and Astronomy, University of California, Los Angeles, CA 90095, USA

⁴ Santa Cruz Institute for Particle Physics and Department of Physics, University of California, Santa Cruz, CA 95064, USA

⁵ Department of Physics, Washington University, St. Louis, MO 63130, USA

⁶ Department of Physics and Astronomy and the Bartol Research Institute, University of Delaware, Newark, DE 19716, USA

⁷ School of Physics and Astronomy, University of Leeds, Leeds, LS2 9JT, UK

⁸ Argonne National Laboratory, 9700 South Cass Avenue, Argonne, IL 60439, USA

⁹ School of Physics, University College Dublin, Belfield, Dublin 4, Ireland

¹⁰ School of Physics, National University of Ireland Galway, University Road, Galway, Ireland

¹¹ Astronomy Department, Adler Planetarium and Astronomy Museum, Chicago, IL 60605, USA

¹² Physics Department, McGill University, Montreal, QC H3A 2T8, Canada

¹³ Department of Physics, Purdue University, West Lafayette, IN 47907, USA

¹⁴ Department of Physics, Grinnell College, Grinnell, IA 50112-1690, USA

¹⁵ Department of Physics and Astronomy, University of Utah, Salt Lake City, UT 84112, USA; cmhui@physics.utah.edu

¹⁶ Enrico Fermi Institute, University of Chicago, Chicago, IL 60637, USA

¹⁷ Department of Physics and Astronomy, Iowa State University, Ames, IA 50011, USA

¹⁸ Department of Physics and Astronomy, University of Iowa, Van Allen Hall, Iowa City, IA 52242, USA

¹⁹ Department of Physics and Astronomy, DePauw University, Greencastle, IN 46135-0037, USA

²⁰ Department of Physics, Pittsburg State University, 1701 South Broadway, Pittsburg, KS 66762, USA

²¹ Department of Physics, Anderson University, 1100 East 5th Street, Anderson, IN 46012, USA

²² Department of Life and Physical Sciences, Galway-Mayo Institute of Technology, Dublin Road, Galway, Ireland

²³ Instituto de Astronomia y Fisica del Espacio, Casilla de Correo 67-Sucursal 28, (C1428ZAA) Ciudad Autónoma de Buenos Aires, Argentina

²⁴ Kavli Institute for Cosmological Physics, University of Chicago, Chicago, IL 60637, USA

²⁵ Department of Applied Physics and Instrumentation, Cork Institute of Technology, Bishopstown, Cork, Ireland

²⁶ Columbia Astrophysics Laboratory, Columbia University, New York, NY 10027, USA

²⁷ Smithsonian Astrophysical Observatory, 60 Garden Street, Cambridge, MA 02138, USA

Received 2009 November 2; accepted 2010 April 26; published 2010 May 21

ABSTRACT

M 87 is a nearby radio galaxy that is detected at energies ranging from radio to very high energy (VHE) gamma rays. Its proximity and its jet, misaligned from our line of sight, enable detailed morphological studies and extensive modeling at radio, optical, and X-ray energies. Flaring activity was observed at all energies, and multi-wavelength correlations would help clarify the origin of the VHE emission. In this paper, we describe a detailed temporal and spectral analysis of the VERITAS VHE gamma-ray observations of M 87 in 2008 and 2009. In the 2008 observing season, VERITAS detected an excess with a statistical significance of 7.2 standard deviations (σ) from M 87 during a joint multi-wavelength monitoring campaign conducted by three major VHE experiments along with the *Chandra X-ray Observatory*. In 2008 February, VERITAS observed a VHE flare from M 87 occurring over a 4 day timespan. The peak nightly flux above 250 GeV was $(1.14 \pm 0.26) \times 10^{-11} \text{ cm}^{-2} \text{ s}^{-1}$, which corresponded to 7.7% of the Crab Nebula flux. M 87 was marginally detected before this 4 day flare period, and was not detected afterward. Spectral analysis of the VERITAS observations showed no significant change in the photon index between the flare and pre-flare states. Shortly after the VHE flare seen by VERITAS, the *Chandra X-ray Observatory* detected the flux from the core of M 87 at a historical maximum, while the flux from the nearby knot HST-1 remained quiescent. Acciari et al. presented the 2008 contemporaneous VHE gamma-ray, *Chandra* X-ray, and Very Long Baseline Array radio observations which suggest the core as the most likely source of VHE emission, in contrast to the 2005 VHE flare that was simultaneous with an X-ray flare in the HST-1 knot. In 2009, VERITAS continued its monitoring of M 87 and marginally detected a 4.2σ excess corresponding to a flux of $\sim 1\%$ of the Crab Nebula. No VHE flaring activity was observed in 2009.

Key words: galaxies: individual (M87, VER J1230+123) – gamma rays: galaxies

Online-only material: color figures

1. INTRODUCTION

M 87 is an FR I radio galaxy located at a distance of 16.7 Mpc near the center of the Virgo cluster. It has been observed at all wavelengths ranging from radio to very high energy (VHE) gamma-rays. Its core is an active galactic nucleus (AGN) powered by a supermassive black hole of mass $(6.0 \pm 0.5) \times 10^9 M_{\odot}$ (Gebhardt & Thomas 2009; see the supporting material of Acciari et al. 2009 for mass corrected distance assumption), which is the source from which the first plasma jet emission was observed (Curtis 1918). Most of the known extragalactic VHE sources are blazars (TeVCat 2007), AGNs with a jet aligned close to the line of sight; in contrast, the jet of M 87 is misaligned. Apparent superluminal motion was observed in both the radio (Cheung et al. 2007) and optical (Biretta et al. 1999) bands for different features along the jet, constraining the jet orientation to less than 30° from the line of sight at the location of the HST-1 knot, which is located $0''.86$ from the core (Harris et al. 2009).

VHE emission from M 87 was first reported by the HEGRA collaboration at a statistical significance of 4.1σ during their 1998–1999 observations (Aharonian et al. 2003). This was confirmed by the HESS collaboration (Aharonian et al. 2006), which additionally reported year-scale flux variability. The observed variability provides a size constraint on the VHE emission production region and disfavors large-scale gamma-ray production models, such as the dark matter annihilation model (Baltz et al. 2000) and the interacting cosmic-ray proton scenario (Pfrommer & Ensslin 2003) which predict steady gamma-ray emission. However, the angular resolution of imaging atmospheric Cherenkov telescopes (IACTs) is insufficient to resolve any structure in M 87. Aharonian et al. (2006) also reported fast (2 day scale) variability during a high state of gamma-ray activity in 2005, which further constrains the VHE emission size and favors the immediate vicinity of the M 87 black hole as the VHE production site; on the other hand, *Chandra* X-ray observations at the time of the VHE flare indicated a different scenario. Strong flux variability from both the core and HST-1 in the energy range 0.2–6 keV has been detected by *Chandra* M 87 monitoring since 2002 (Harris et al. 2003). At the same period of the flare observed by HESS in 2005, Harris et al. (2008) reported an X-ray flux from HST-1 at more than 50 times the intensity observed in 2000, along with flaring activity observed in ultraviolet and radio wavelengths, suggesting the HST-1 knot as a more likely source of VHE emission than the core.

The All-Sky Monitor (ASM) on *RXTE* has provided daily monitoring of M 87 in the energy range 2–12 keV since 1996. However, ASM cannot resolve the core and the HST-1 knot. A year-scale correlation between the annual ASM/*RXTE* X-ray flux and the VHE gamma-ray flux recorded over the past 10 years was reported by Acciari et al. (2008). The core was presented as the more favorable VHE production site over HST-1 based on this year-scale correlation, and the non-detection of the 2005 flare in the HST-1 knot by ASM. However, no year-scale correlation has been seen with *Chandra* data of the M 87 core or the HST-1

knot over the past five years in the 0.2–6 keV range. The ASM/*RXTE* quick-look results do not show any correlated activity with VHE observations at shorter timescales, as a result of the limited sensitivity of ASM.

The proximity of M 87 and its misaligned jet enable high-resolution studies of its jet structures in radio, optical, and X-rays (Marshall et al. 2002; Perlman & Wilson 2005). The jet morphology is similar in those wavebands, and leptonic synchrotron radiation is favored as the process for non-thermal emission within the jet (Wilson & Yang 2002). Based on the multi-wavelength correlated activities and variability studies, the favored candidate for VHE emission is the small-scale (sub-arcsecond) jet region. Reimer et al. (2004) propose a synchrotron proton blazar model in which protons are accelerated to energies above EeV and emit gamma rays via muon/pion synchrotron or proton synchrotron radiation. However, this model requires a strong magnetic field to accelerate the protons to such high energies, and the predicted VHE spectrum is steeper than observed. Several leptonic models involving synchrotron and inverse Compton (IC) radiation have also been suggested, with the multi-component emission originating in the inner jet. There is the model by Georganopoulos et al. (2005) in which energetic electrons IC scatter off of synchrotron photons produced downstream in the decelerating jet, a scenario by Lenain et al. (2008) in which VHE emission is produced via the synchrotron self-Compton (SSC) process inside several similar homogenous compact components that contain more energetic electrons than the jet, and the model by Tavecchio & Ghisellini (2008) in which a fast-moving spine is surrounded by a slower-moving sheath producing VHE emission via external-Compton scattering. Single-component SSC emission is recently modeled by Abdo et al. (2009) with Very Long Baseline Array (VLBA) radio, *Chandra* X-ray, and *Fermi*-LAT 2009 data. However, comparing the model to archival non-flaring VHE data, it appears to underpredict the VHE emission.

The vicinity of the black hole (the core) has been suggested by Levinson (2000) and Neronov & Aharonian (2007) in the black hole magnetosphere model, in which gamma-ray photons are produced by electrons accelerated by the electromagnetic field of the black hole. The HST-1 knot, $0''.86$ away from the core, has also been demonstrated as a possible location for jet reconfinement where photons can be upscattered to TeV energies via IC process (Stawarz et al. 2006).

In 2008, the VHE gamma-ray experiments HESS, MAGIC, and VERITAS took part in a joint multi-wavelength monitoring campaign of M 87 along with *Chandra* (Beilicke et al. 2008). The VHE observations were closely coordinated in order to guarantee a reasonable coverage around the *Chandra* pointings and a well-sampled VHE light curve during the first half of 2008. During this joint monitoring campaign, MAGIC reported flaring activities during a 13 day observation period between January 30 (MJD 54495) and February 11 (MJD 54507), with day-scale variability occurring throughout the duration of the flare (Albert et al. 2008). Subsequently, the VERITAS collaboration triggered intensified observations of M 87, and detected a 4 day flare from February 9 (MJD 54505) to February 13 (MJD 54509). The VHE and *Chandra* X-ray light curves of the joint campaign, along with a coincident VLBA radio light curve, are presented in Acciari et al. (2009), which also includes a discussion on the radio/VHE gamma-ray correlation as evidence that the VHE emission originates from the core.

The VHE flux monitoring campaign continued in 2009 with MAGIC and VERITAS. In this paper, we present the results

²⁸ Now at the Laboratoire Leprince-Ringuet, Ecole Polytechnique, CNRS/IN2P3, F-91128 Palaiseau, France.

²⁹ Now at the DESY, Platanenallee 6, 15738 Zeuthen, Germany.

³⁰ Now at the Department of Physics, Anderson University, 1100 East 5th Street, Anderson, IN 46012, USA.

³¹ Now at the Institut für Physik und Astronomie, Universität Potsdam, 14476 Potsdam-Golm, Germany; DESY, Platanenallee 6, 15738 Zeuthen, Germany.

³² Now at the Los Alamos National Laboratory, MS H803, Los Alamos, NM 87545, USA.

Table 1

M 87 Differential Flux Measured Between 2007 December and 2008 May by VERITAS

Energy (TeV)	Differential Flux ($\text{cm}^{-2} \text{s}^{-1} \text{TeV}^{-1}$)	Significance (σ)
0.24	$(1.99 \pm 0.54) \times 10^{-11}$	3.68
0.42	$(3.56 \pm 1.16) \times 10^{-12}$	3.07
0.75	$(1.51 \pm 0.34) \times 10^{-12}$	4.44
1.33	$(1.70 \pm 0.95) \times 10^{-13}$	1.79
2.37	$(6.02 \pm 3.40) \times 10^{-14}$	1.78
4.22	$(1.72 \pm 1.13) \times 10^{-14}$	1.52

from two seasons (2008–2009) of VERITAS observations, along with a full analysis on the timescale of the flux variability, and a search for spectral variability in the 2008 data set when the VHE flaring activity was observed.

2. OBSERVATIONS AND ANALYSIS

VERITAS is an array of four 12 m diameter IACTs located at the Fred Lawrence Whipple Observatory on Mount Hopkins ($31^{\circ}40' \text{ N}$, $110^{\circ}57' \text{ W}$) at an altitude of 1.3 km above sea level. Each telescope has a total area of 110 m^2 and an f/D ratio of 1.0. Each telescope camera is equipped with 499 photomultiplier tubes, arranged in a hexagonal lattice covering a field of view (FOV) of $3^{\circ}5'$. The array is sensitive from $\sim 100 \text{ GeV}$ to more than 30 TeV, with an effective area of up to 10^5 m^2 and an angular resolution of $0^{\circ}.1$ at 1 TeV (68% containment). VERITAS can detect a source with 1% Crab Nebula flux in less than 50 hr, and a source with 5% Crab Nebula flux in ~ 2.5 hr. For more technical details of VERITAS, see Holder et al. (2006).

M 87 was observed with VERITAS for over 43 hr between 2007 December and 2008 May and over 25 hr between 2009 January and May, at a range of zenith angles from 19° to 41° . All 2008 data and 81% of 2009 data used were taken with four telescopes, while 19% of 2009 data were taken with only a three-telescope array. After eliminating observations in poor weather and those with an unstable trigger rate, 37 hr and 19 hr of good-quality live time remain in 2008 and 2009, respectively.

Shower images from all working telescopes are first corrected in gain and timing using parameters obtained from the nightly laser calibration data (Hanna et al. 2008). The images are then passed through a two-step cleaning process that retains pixels with a signal that is several times higher than the night-sky background level. Each shower image is then parameterized (Hillas 1985) and the shower direction is reconstructed using the stereoscopic technique (Hofmann et al. 1999). Events are then selected as gamma-ray-like if at least three camera images pass the standard cuts optimized for a 10% Crab Nebula flux source (Colin et al. 2008). All the observations were performed in “wobble mode” where M 87 was tracked with a $0^{\circ}.5$ offset relative to the camera such that the camera’s FOV contain both the source region and regions for background estimation. The on-source region is defined by a $0^{\circ}.15$ radius circle centered on the M 87 core. All gamma-ray-like events within this region are summed as the ON count, and the background estimated from seven identically sized regions reflected from the source region around the camera center is summed as the OFF count (Berge et al. 2007). The ON and OFF counts are then used in Formula (17) of Li & Ma (1983) to calculate the significance of the excess. As a standard procedure in VERITAS, the results were confirmed by at least one independent analysis package (Daniel et al. 2008) which was presented in Acciari et al. (2009).

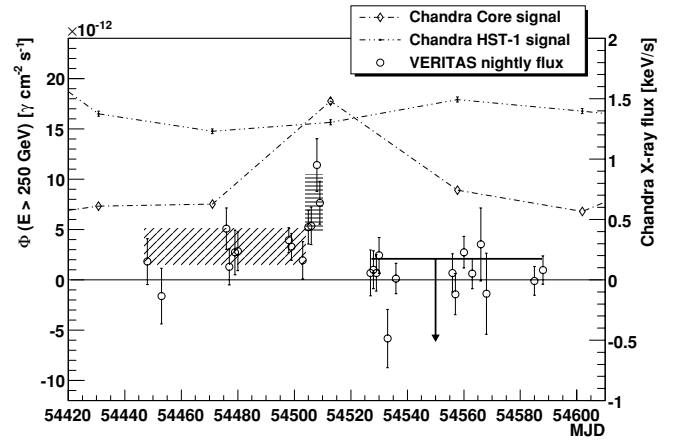


Figure 1. VERITAS night-by-night VHE gamma-ray flux and *Chandra* X-ray flux (Harris et al. 2009) from the core and from the HST-1 knot of M 87 in 2008. The flare period (MJD 54505–54509, February 9–13) seen in VHE gamma-rays coincides with a historically high state of the core in X-rays, while the HST-1 knot remains in a low flux state. The black slant-lined area shows the 99% confidence intervals of the pre-flare period, the black horizontal-lined area shows the 99% confidence intervals of the flare period, and the black line with the arrow indicates the upper limit of the post-flare period at 99% confidence level (Helene 1983).

3. RESULTS

3.1. 2008

The VERITAS observations in 2008 resulted in 450 excess events, corresponding to a statistical significance of 7.2σ . The average flux above 250 GeV is $(2.74 \pm 0.61) \times 10^{-12} \text{ cm}^{-2} \text{ s}^{-1}$, corresponding to 1.8% of the Crab Nebula flux. The differential energy spectrum of M 87 measured by VERITAS in 2008 is consistent with a power-law distribution $dN/dE = \Phi_0(E/\text{TeV})^{-\Gamma}$, with $\Phi_0 = (5.17 \pm 0.91_{\text{stat}} \pm 1.03_{\text{stat}}) \times 10^{-13} \text{ cm}^{-2} \text{ s}^{-1} \text{ TeV}^{-1}$ and $\Gamma = 2.49 \pm 0.19_{\text{stat}} \pm 0.20_{\text{syst}}$. The χ^2/dof for the power-law fit is 3.1/4.0. The measured photon index is consistent with reported measurements from Aharonian et al. (2006), Acciari et al. (2008), and Albert et al. (2008) ranging from 2.22 to 2.62 with statistical uncertainties between 0.11 and 0.35. Table 1 lists the differential flux points measured by VERITAS in 2008.

The 2008 VERITAS light curve is shown in Figure 1 assuming the average fitted photon index of 2.50. The χ^2/dof of a constant rate fit to the entire data set is 52/26, rejecting the constant flux hypothesis at 99.9% confidence level. On February 9 (MJD 54505), M 87 was detected at over 4σ after 2 hr of observation and a trigger alert was sent out to other collaborations for intensified observations. The peak flux of the VERITAS data set occurred on the night of February 12 (MJD 54508) at $(1.14 \pm 0.26) \times 10^{-11} \text{ cm}^{-2} \text{ s}^{-1}$ above 250 GeV, equivalent to 7.7% of the Crab Nebula flux. The flare period is defined by the nights removed from the whole data set such that the constant rate fit to the rest of the light curve reaches a χ^2/dof close to 1. The nights that meet the criteria for the flare period are February 9, 10, 12, and 13 (MJD 54505–54509). The data set is then further split into pre-flare and post-flare periods.

During the flare period, M 87 was observed for 5.4 hr of live time and was detected at 7.4σ (pre-trials). The flux above 250 GeV during the flare period was $(7.59 \pm 1.11) \times 10^{-12} \text{ cm}^{-2} \text{ s}^{-1}$, corresponding to 5.1% of the Crab Nebula flux. The 99% confidence interval for the flux during the flare period (see horizontal-lined area between MJD 54505 and 54509 in Figure 1) is between $4.73 \times 10^{-12} \text{ cm}^{-2} \text{ s}^{-1}$ and $10.45 \times 10^{-12} \text{ cm}^{-2} \text{ s}^{-1}$.

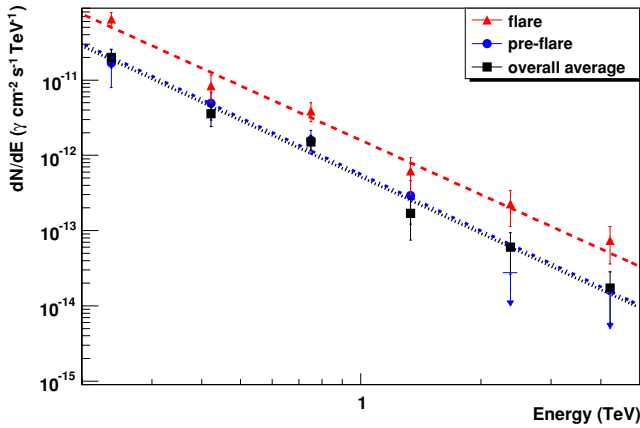


Figure 2. Spectra of M 87 measured at different periods by VERITAS. Data points less than 1.5σ are represented as upper limits. The power-law fit parameters are listed in Table 2. The photon energy distribution is consistent throughout different activity levels, and there is no indication of a spectral cutoff. (A color version of this figure is available in the online journal.)

Table 2
Power-law Fit Parameters of the VHE Spectrum of M 87 in Different Epochs During 2008

Data Set	Φ_0 ($10^{-13} \text{ cm}^{-2} \text{ s}^{-1} \text{ TeV}^{-1}$)	Γ	χ^2/dof
2008 overall	5.2 ± 0.9	2.5 ± 0.2	3.1/4
Flare state	15.9 ± 2.9	2.4 ± 0.2	3.9/4
Pre-flare state	5.6 ± 1.5	2.5 ± 0.3	1.3/4

Before the flare period (MJD 54448–54503), which included two nights immediately after the major flare observed by MAGIC (Albert et al. 2008), M 87 was marginally detected with 13.8 hr of live time at a flux of $(3.30 \pm 0.68) \times 10^{-12} \text{ cm}^{-2} \text{ s}^{-1}$ above 250 GeV. The 99% confidence interval for the flux during the pre-flare period (see slant-lined area between MJD 54448 and 54503 in Figure 1) is between $1.55 \times 10^{-12} \text{ cm}^{-2} \text{ s}^{-1}$ and $5.05 \times 10^{-12} \text{ cm}^{-2} \text{ s}^{-1}$. M 87 was observed for an additional 17.2 hr of live time after the flare period and was not detected. An upper limit of $2.1 \times 10^{-12} \text{ cm}^{-2} \text{ s}^{-1}$ at 99% confidence level (Helene 1983) is established for the post-flare period, corresponding to 1.4% of the Crab Nebula flux. Assuming a normal distribution for the flux measurement, the flare flux is higher than the pre-flare flux at 99.95% confidence level, and the pre-flare flux is higher than the post-flare flux at 99.8% confidence level. All of the above calculations were performed under the assumption of a constant photon index of 2.50.

The spectra from different periods are plotted in Figure 2 and there is no indication of a spectral cutoff. The power-law fit parameters from the overall, flare, and pre-flare spectra are displayed in Table 2. No significant difference in photon index and photon energy distribution is found between the flare and pre-flare states.

To test if there is any correlation between the spectral flux and photon index measured during different activity levels corresponding to the core, a linear test function of the form $\Gamma = p_0 + p_1 \times \log_{10} \Phi_0$ was fitted to past measurements by Aharonian et al. (2006) in 2004 and Acciari et al. (2008) in 2007, and the high/low states measured by Albert et al. (2008) and by VERITAS in 2008 (see Figure 3). The measurement by HESS in 2005 is excluded in the fit due to possible contamination from the HST-1 flare. The χ^2/dof of the linear fit is 1.7/4 and the corresponding probability of a correlation between photon index and flux is 78.6%. The fit parameter p_1 is consistent with

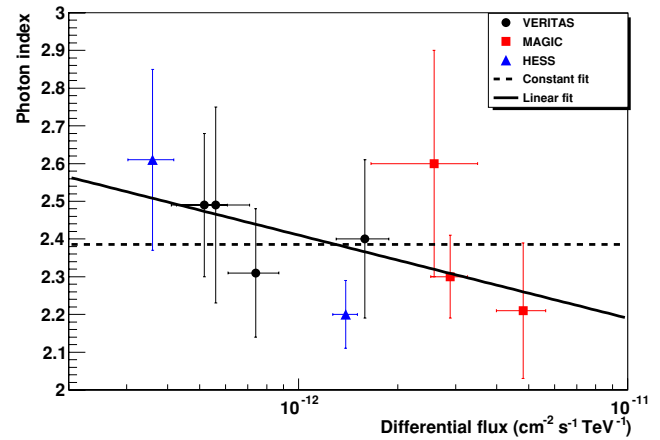


Figure 3. Photon index vs. differential flux as reported by HESS in 2004 and 2005 (Aharonian et al. 2006), by MAGIC in 2008 (overall, flare, and non-flare; Albert et al. 2008), and by VERITAS in 2007 (Acciari et al. 2008) and 2008 (overall, flare, and pre-flare). All spectra are compatible within their statistical errors. A linear correlation fit between photon index and flux has the same probability as a constant photon index fit. (A color version of this figure is available in the online journal.)

zero. Fitting a constant photon index gave a χ^2/dof of 2.7/5 and a corresponding probability of 74.6%. No significant correlation is found between the photon index and the flux.

At the time of the flare detected by VERITAS, *Chandra* measured the core X-ray flux at a historical maximum, at 4.1σ above the mean core flux between 2000 and 2009, and exceeding the flux from the HST-1 knot (see Figures 1 and 4; Harris et al. 2009). The peak core X-ray flux measured by *Chandra* during the observation period of VERITAS was 2.3 times the average core X-ray flux, with the average calculated excluding this flare data point. While the HST-1 knot X-ray flux during this period fluctuated $\pm 10\%$ from the average and is relatively steady when compared to the core emission. Figure 5 shows the fractional change per year (fpy) first presented in Harris et al. (2009). Around the 2008 VHE gamma-ray flare period, the *Chandra* core fpy is more variable than that of the *Chandra* HST-1 fpy measurement. The definition of fpy is repeated below (Harris et al. 2009):

$$\text{fpy} = \frac{I_2 - I_1}{I_i \Delta t}, \quad (1)$$

$$\sigma_{\text{fpy}} = \frac{1}{\Delta t} \times \frac{I_j}{I_i} \times \sqrt{\left(\frac{\sigma_1}{I_1}\right)^2 + \left(\frac{\sigma_2}{I_2}\right)^2}, \quad (2)$$

where I is the X-ray intensity measured by *Chandra* and Δt is the time between the two intensity measurements in units of year. If the X-ray intensity is increasing (i.e., $I_2 > I_1$), then $i = 1$ and $j = 2$; if the X-ray intensity is decreasing (i.e., $I_2 < I_1$), then $i = 2$ and $j = 1$.

3.2. 2009

The VERITAS observations in 2009 resulted in 134 excess events at a significance of 4.2σ . The χ^2/dof of a constant rate fit to the entire data set is 23/18 and no significant variability was observed in the 2009 data set. The average flux above 250 GeV is $(1.59 \pm 0.39) \times 10^{-12} \text{ cm}^{-2} \text{ s}^{-1}$ assuming a photon index of 2.50. This corresponds to 1.1% of the Crab Nebula flux and is consistent with the reported *Fermi*-LAT spectrum (Abdo et al. 2009). The 2009 flux is below the 2008 pre-flare flux at the 98.5% confidence level, but above the 2008 post-flare flux at the 87.6% confidence level. Figure 5 shows the light curves of

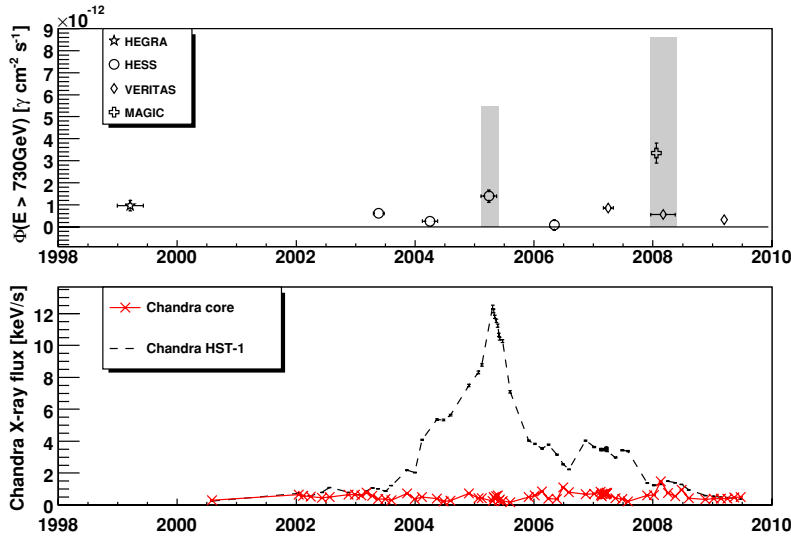


Figure 4. M 87 yearly VHE gamma-ray (Aharonian et al. 2003, 2006; Acciari et al. 2008; Albert et al. 2008) and X-ray fluxes (Harris et al. 2009). The VHE gamma-ray flux is for energy >730 GeV due to the original flux scale used in the HEGRA paper. This yearly flux plot is first presented in Acciari et al. (2008) and is now updated with 2008 and 2009 data. Gray areas represent the range of variable VHE fluxes observed that year to give a more accurate picture of the flux level of M 87.

(A color version of this figure is available in the online journal.)

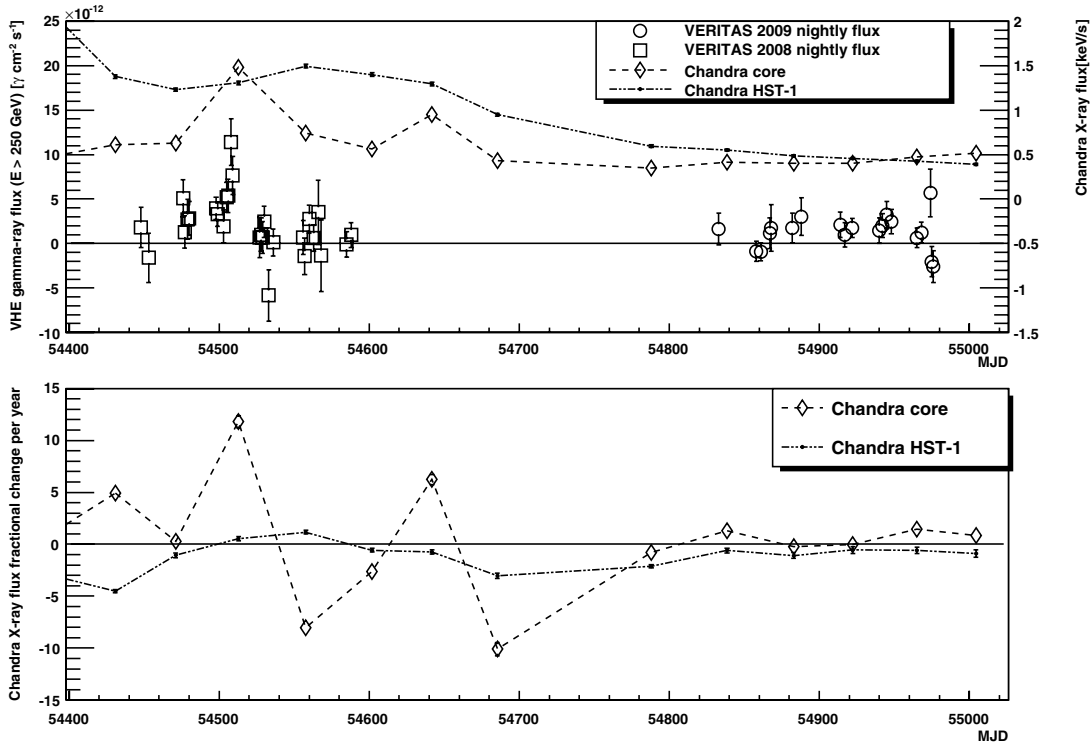


Figure 5. Upper panel: VERITAS night-by-night VHE gamma-ray flux and *Chandra* X-ray flux from the core and from the HST-1 knot of M 87 in 2008 (Harris et al. 2009) and 2009. Lower panel: *Chandra* X-ray flux fpy, see the text for definition (Harris et al. 2009).

both 2008 and 2009 observed by VERITAS and the X-ray flux measured by *Chandra* for the core and the knot HST-1, along with the fpy of *Chandra* X-ray flux.

During the 2009 observation period, *Chandra* took a flux measurement every 40–50 days. The HST-1 flux measured by *Chandra* is steadily declining at a rate of 5%–10% when compared to the previous flux ($\delta I/I_1$). The core flux, however, is mostly increasing by as much as 18%. The lack of VHE activity during this period suggests a possible association between VHE flares and significant changes in the X-ray flux such as the one seen in 2008 where the core fpy is more variable than in 2009 (see Figure 5).

4. DISCUSSION

The proximity of M 87 and its misaligned jet have enabled the study of its jet morphology in a broad range of energies. Flaring activities from individual jet features have been observed in radio, optical, and X-rays in parallel (Cheung et al. 2007). Modeling of the particle acceleration yields several possible VHE emission origins. Even though the VHE gamma-ray technique cannot resolve individual features of M 87, the rapid variability reported by Aharonian et al. (2006) and Albert et al. (2008) has constrained the size of the VHE emission region to $<2.6\delta R_s$, where δ is the relativistic Doppler factor and R_s is the Schwarzschild radius of the M 87 black hole

($R_s \sim 10^{15}$ cm). During the 2008 joint monitoring campaign of M 87, VERITAS observed a gamma-ray flare in 2008 February which spanned 4 days, constraining the emission region size to $R \leq R_{\text{var}} = \delta c \Delta t / (1+z) \approx \delta \times 10^{16}$ cm. Radio observations have shown evidence that charged particles are accelerated in the immediate vicinity of the black hole closer than $100 R_s$ (Acciari et al. 2009). Combining these radio observations with the size constraint from the VERITAS 2008 data, we can constrain the relativistic Doppler factor $\delta \leq 10$ with the flaring activity measured by VERITAS.

The VHE emission size constraint narrows down the most probable VHE emission location to either the unresolved core region or the HST-1 knot. X-ray timescale analysis presented by Harris et al. (2009) suggests the X-ray emission size of the core to be smaller than that of HST-1. However, the upper limits on the X-ray emission region size from the timescale analysis are still larger than the VHE emission size inferred from the VHE variability timescales reported previously. Therefore, both the HST-1 and the core region remain as the possible origins of VHE emission.

In 2009, VERITAS detected M 87 similar to the 2008 pre-flare level. The X-ray timescale analysis is repeated for the 2009 *Chandra* data and the fpy for the core in 2009 is smaller than in 2008 during the VHE gamma-ray flare. The fpy of the knot HST-1 appeared to be negative throughout 2008 and 2009, and at a smaller amplitude than the core. This may be an indication of correlation between large X-ray flux changes and flaring activities in VHE gamma-rays. It should be noted, however, that large fpy in the core was observed by *Chandra* as well in 2007 with no corresponding VHE gamma-ray flare. A similar analysis is not performed for the 2005 HESS flare due to contamination from the knot HST-1 in *Chandra* data.

The compactness of the particle accelerators operating in the vicinity of the supermassive black hole and the absence of a significant cutoff in the spectrum imply that the particle acceleration mechanism is highly efficient. Levinson (2000), Neronov & Aharonian (2007), and others have argued that acceleration mechanisms similar to those in pulsar magnetosphere models can also operate in the black hole magnetosphere. The black hole magnetosphere model and the two-zone leptonic models (Georganopoulos et al. 2005; Lenain et al. 2008; Tavecchio & Ghisellini 2008) can reproduce the VHE spectrum and the flux variability well. While no constraints can be placed on the VHE range of these models, since VERITAS and other VHE gamma-ray instruments did not observe a cutoff in the spectrum of M 87, the *Fermi Gamma-ray Telescope*, sensitive from MeV to GeV energies, can potentially provide constraints on the magnetic field strength and a measure of low-energy gamma-ray photon flux from the synchrotron/curvature radiation. Abdo et al. (2009) presented the first year of *Fermi*-LAT observations of M 87 in 2009 during its quiescent state. Continual monitoring in all wavelengths is essential for the modeling of the spectral energy distribution of M 87. Future instruments such as CTA/AGIS, with their improved sensitivity, can potentially detect shorter timescale variability and further constrain the size of the VHE emission region.

Begelman (2009) provided a concise commentary on the M 87 2008 multi-wavelength results and the importance of multi-wavelength observations to understanding particle acceleration mechanisms near black holes. The high-resolution imaging of radio telescopes, combined with the VHE gamma-ray observations from ground-based instruments, have shown the first association between a VHE gamma-ray flare and an increase in radio flux coming from a region very close to the black hole

(Acciari et al. 2009). This coincident multi-wavelength coverage led to several modeling discussions of the joint VHE and radio light curves (see the supplement of Acciari et al. 2009). Even with M 87 day-scale VHE flux variability and additional constraints from radio and X-ray observations, several plausible models remain, which explain how particles are accelerated to very high energies near the black hole and how the consequent radiation is able to reach us. Multi-wavelength monitoring work is being continued, and is essential to address these questions.

VERITAS is supported by grants from the US Department of Energy, the US National Science Foundation, and the Smithsonian Institution, by NSERC in Canada, by Science Foundation Ireland, and by STFC in the UK.

The *Chandra* M 87 monitoring work at SAO was supported by NASA grants GO8-9116X and GO90108X.

F. Massaro acknowledges the Foundation BLANCEFLOR Boncompagni-Ludovisi, née Bildt for the grant awarded him in 2009 to support his research.

Facilities: CXO, HEGRA, HESS, MAGIC, VERITAS

REFERENCES

- Abdo, A. A., et al. 2009, *ApJ*, 707, 55
 Acciari, V. A., et al. 2008, *ApJ*, 679, 397
 Acciari, V. A., et al. 2009, *Science*, 325, 444
 Aharonian, F., et al. 2003, *A&A*, 403, L1
 Aharonian, F., et al. 2006, *Science*, 314, 1424
 Albert, J., et al. 2008, *ApJ*, 685, L23
 Baltz, E. A., Briot, C., Salati, P., Taillet, R., & Silk, J. 2000, *Phys. Rev. D*, 61, 023514
 Begelman, M. 2009, *Science*, 325, 399
 Beilicke, M., et al. 2008, in AIP Conf. Proc. 1085, High Energy Gamma-ray Astronomy, ed. F. A. Aharonian, W. Hofmann, & F. Rieger (Melville, NY: AIP), 553
 Berge, D., Funk, S., & Hinton, J. 2007, *A&A*, 466, 1219
 Biretta, J. A., Sparks, W. B., & Macchetto, F. 1999, *ApJ*, 520, 621
 Cheung, C. C., Harris, D. E., & Stawarz, L. 2007, *ApJ*, 663, L65
 Colin, P., et al. 2008, in ICRC 3: Proc. 30th International Cosmic Ray Conf., ed. R. Caballero et al. (Mexico City: Universidad Nacional Autónoma de México), 997
 Curtis, H. D. 1918, *Publ. Lick Obs.*, 13, 9
 Daniel, M. K., et al. 2008, in ICRC 3: Proc. 30th International Cosmic Ray Conf., ed. R. Caballero et al. (Mexico City: Universidad Nacional Autónoma de México), 1325
 Gebhardt, K., & Thomas, J. 2009, *ApJ*, 700, 1690
 Georganopoulos, M., Perlman, E. S., & Kazanas, D. 2005, *ApJ*, 634, L33
 Hanna, D., et al. 2008, in ICRC 3: Proc. 30th International Cosmic Ray Conf., ed. R. Caballero et al. (Mexico City: Universidad Nacional Autónoma de México), 1417
 Harris, D. E., Biretta, J. A., Junor, W., Perlman, E. S., Sparks, W. B., & Wilson, A. S. 2003, *ApJ*, 586, L41
 Harris, D. E., Cheung, C. C., Stawarz, L., Biretta, J. A., & Perlman, E. S. 2009, *ApJ*, 699, 305
 Harris, D. E., Cheung, C. C., Stawarz, L., Biretta, J. A., Sparks, W., Perlman, E. S., & Wilson, A. S. 2008, in ASP Conf. Ser. 386, Extragalactic Jets, ed. T. A. Rector & D. S. De Young (San Francisco, CA: ASP), 80
 Helene, O. 1983, *Nucl. Instrum. Methods Phys. Res.*, 212, 319
 Hillas, A. M. 1985, 19th ICRC Proc., 3, 445
 Hofmann, W., et al. 1999, *Astropart. Phys.*, 12, 135
 Holder, J., et al. 2006, *Astropart. Phys.*, 25, 391
 Lenain, J.-P., Boisson, C., Sol, H., & Katarzynski, K. 2008, *A&A*, 478, 111
 Levinson, A. 2000, *Phys. Rev. Lett.*, 85, 5
 Li, T. P., & Ma, Y. Q. 1983, *ApJ*, 272, 317
 Marshall, H. L., et al. 2002, *ApJ*, 564, 683
 Neronov, A., & Aharonian, F. A. 2007, *ApJ*, 671, 85
 Perlman, E. S., & Wilson, A. S. 2005, *ApJ*, 627, 140
 Pfrommer, C., & Ensslin, T. A. 2003, *A&A*, 407, L73
 Reimer, A., Protheroe, R. J., & Donea, A.-C. 2004, *A&A*, 419, 89
 Stawarz, L., Aharonian, F., Kataoka, J., Ostrowski, M., Siemiginowska, A., & Sikora, M. 2006, *MNRAS*, 370, 981
 Tavecchio, F., & Ghisellini, G. 2008, *MNRAS*, 385, L98
 TeVCat 2007, Online Gamma-Ray Catalog (<http://tevcat.uchicago.edu>)
 Wilson, A. S., & Yang, Y. 2002, *ApJ*, 568, 133